AIAA-99-1470

NONLINEAR AEROELASTICITY AND FLIGHT DYNAMICS OF HIGH-ALTITUDE LONG-ENDURANCE AIRCRAFT

Mayuresh J. Patil[*], **Dewey H. Hodges**[†]
Georgia Institute of Technology, Atlanta, Georgia
and
Carlos E. S. Cesnik[‡]
Massachusetts Institute of Technology, Cambridge, Massachusetts

Abstract

High-Altitude Long-Endurance (HALE) aircraft have wings with high aspect ratios. During operations of these aircraft, the wings can undergo large deflections. These large deflections can change the natural frequencies of the wing which, in turn, can produce noticeable changes in its aeroelastic behavior. This behavior can be accounted for only by using a rigorous nonlinear aeroelastic analysis. Results are obtained from such an analysis for aeroelastic behavior as well as overall flight dynamic characteristics of a complete aircraft model representative of HALE aircraft. When the nonlinear flexibility effects are taken into account in the calculation of trim and flight dynamics characteristics, the predicted aeroelastic behavior of the complete aircraft turns out to be very different from what it would be without such effects. The overall flight dynamic characteristics of the aircraft also change due to wing flexibility. For example, the results show that the trim solution as well as the short-period and phugoid modes are affected by wing flexibility.

Introduction

High-Altitude Long-Endurance (HALE) aircraft have gained importance over the past decade. Unmanned HALE aircraft are being designed for a variety of flight missions including environmental sensing, military reconnaissance and cellular telephone relay. HALE aircraft have high-aspect-ratio wings. To make the concept feasible in terms of weight restrictions, the wings are very flexible. Wing flexibility coupled with the long length leads to the possibility of large deflections during normal flight operation. Also, to fly at high altitudes and low speeds requires operation at high angles of attack, likely close to stall. Thus, it is unlikely that an aeroelastic analysis based on linearization about the undeformed wing could lead to reliably accurate aeroelastic results. Even the trim condition and flight dynamic frequencies could be significantly affected by the flexibility and nonlinear deformation.

Nonlinear aeroelastic analysis has gathered a lot of momentum in the last decade due to understanding of nonlinear dynamics as applied to complex systems and the availability of the required mathematical tools. The studies conducted by Dugundji and his co-workers are a combination of analysis and experimental validation of the effects of dynamic stall on aeroelastic instabilities for simple cantilevered laminated plate-like wings.[2] ONERA stall model was used for aerodynamic loads.

Tang and Dowell have studied the flutter and forced response of a flexible rotor blade.[3] In this study, geometrical structural nonlinearity and free-play structural nonlinearity is taken into consideration. Again, high-angle-of-attack unsteady aerodynamics was modeled using the ONERA dynamic stall model.

Virgin and Dowell have studied the nonlinear behavior of airfoils with control surface free-play and investigated the limit-cycle oscillations and chaotic motion of airfoils.[4] Gilliatt, Strganac and Kurdila have investigated the nonlinear aeroelastic behavior of an airfoil experimentally and analytically.[5] A nonlinear sup-

[*]Graduate Research Assistant, School of Aerospace Engineering Member, AIAA.

[†]Professor, School of Aerospace Engineering, Fellow, AIAA. Member, AHS.

[‡]Assistant Professor of Aeronautics and Astronautics. Senior Member, AIAA. Member, AHS.

Presented at the 40th Structures, Structural Dynamics and Materials Conference, St.Louis, Missouri, April 12 – 15, 1999

port mechanism was constructed and is used to represent continuous structural nonlinearities.

Aeroelastic characteristics of highly flexible aircraft was investigated by van Schoor and von Flotow.[6] The complete aircraft was modeled using a few modes of vibration, including rigid-body modes. Waszak and Schmidt[7] used Lagrange's equations to derive the nonlinear equations of motion for a flexible aircraft. Generalized aerodynamic forces are added as closed-form integrals. This form helps in identifying the effects of various parameters on the aircraft dynamics.

Linear aeroelastic and flight dynamic analysis results for a HALE aircraft are presented by Pendaries.[8] The results highlight the effect of rigid body modes on wing aeroelastic characteristics and the effect of wing flexibility on the aircraft flight dynamic characteristics.

The present study presents the results obtained using a low-order, high-fidelity nonlinear aeroelastic analysis. A theoretical basis has been established for a consistent analysis which takes into account, *i)* material anisotropy, *ii)* geometrical nonlinearities of the structure, *iii)* unsteady flow behavior, and *iv)* dynamic stall. The formulation and preliminary results for the nonlinear aeroelastic analysis of an aircraft has been presented in an earlier paper.[1] The present paper is essentially a continuation of the earlier work and presents more results specific to HALE aircraft. The results obtained give insight into the effects of the structural geometric nonlinearities on the trim solution, flutter speed, and flight dynamics.

Present Model

The present theory is based on two separate works, viz., *i)* mixed variational formulation based on the exact intrinsic equations for dynamics of beams in moving frames[9] and *ii)* finite-state airloads for deformable airfoils on fixed and rotating wings.[10, 11] The former theory is a nonlinear intrinsic formulation for the dynamics of initially curved and twisted beams in a moving frame. There are no approximations to the geometry of the reference line of the deformed beam or to the orientation of the cross-sectional reference frame of the deformed beam. A compact mixed variational formulation can be derived from these equations which is well-suited for low-order beam finite element analysis based in part on the original paper by Hodges.[9] The latter work presents a state-space theory for the lift, drag, and all generalized forces of a deformable airfoil. Trailing edge flap deflections are included indirectly as a special case of generalized deformation. The model is based on thin-airfoil theory and allows for arbitrary small deformations of the airfoil fixed in a reference frame which can perform arbitrary large motions. A more detailed formulation of the aeroservoelastic analysis of a complete aircraft is given in an earlier paper by Patil, Hodges and Cesnik.[1]

By coupling the structural and aerodynamics models one gets the complete aeroelastic model. By selecting the shape functions for the variational quantities in the formulation, one can choose between, *i)* finite elements in space leading to a set of ordinary nonlinear differential equations in time, *ii)* finite elements in space and time leading to a set of nonlinear algebraic equations. Using finite elements in space one can obtain the steady-state solution and can calculate linearized equations of motion about the steady state for stability analysis. This state space representation can also be used for linear robust control synthesis. Space-time finite elements are used for time marching and thus study the dynamic nonlinear behavior of the system. This kind of analysis is useful in finding the amplitudes of the limit cycle oscillations if the system is found unstable.

Thus, three kinds of solutions are possible: *i)* a nonlinear steady-state solution, *ii)* a stability analysis based on linearization about the steady state, *ii)* and a time-marching solution for nonlinear dynamics of the system.

Results

Table 1 gives the structural and planform data for the aircraft model under investigation. Though the data were obtained by modifying Daedalus data it is representative of the HALE kind of design. In this section linear structural dynamics and aeroelasticity results will be presented and compared with published data. Next, results with nonlinearities included are presented to show their importance. These include natural frequencies, flutter frequencies and speeds, and loci of roots, all obtained for an analysis linearized about an equilibrium configuration calculated from a fully nonlinear analysis.

Linear results

Table 2 presents frequency results based on theories which are linearized about the undeformed state, i.e., the usual linear approach. The results for the present wing model were obtained using eight finite elements with all nonlinear effects suppressed. They are compared against the results obtained by theory of Ref. 12

WING	
Half span	16 m
Chord	1 m
Mass per unit length	0.75 kg/m
Mom. Inertia (50% chord)	0.1 kg m
Spanwise elastic axis	50% chord
Center of gravity	50% chord
Bending rigidity	2×10^4 N m^2
Torsional rigidity	1×10^4 N m^2
Bending rigidity (chordwise)	4×10^6 N m^2
PAYLOAD & TAILBOOM	
Mass	50 kg
Moment of Inertia	200 kg m^2
Length of tail boom	10 m
TAIL	
Half span	2.5 m
Chord	0.5 m
Mass per unit length	0.08 kg/m
Moment of Inertia	0.01 kg m
Center of gravity	50 % of chord
FLIGHT CONDITION	
Altitude	20 km
Density of air	0.0889 kg/m^3

Table 1: Aircraft model data

	Present Analysis	Analysis of Ref. 12	% Error
1^{st} Flat. Bend.	2.247	2.243	+0.2
2^{nd} Flat. Bend.	14.606	14.056	+3.9
3^{rd} Flat. Bend.	44.012	39.356	+11.8
1^{st} Torsion	31.146	31.046	+0.3
1^{st} Edge. Bend.	31.739	31.718	+0.1

Table 2: Comparison of linear frequency results

	Present Analysis	Analysis of Ref. 12	% Diff.
Flut. Speed	32.21	32.51	-0.9
Flut. Freq.	22.61	22.37	+1.1
Div. Speed	37.29	37.15	+0.4

Table 3: Comparison of linear aeroelastic results

which gives exact results for frequencies of a beam with torsion, flatwise bending, and edgewise bending. The frequencies are very close except for the third flatwise bending mode, which does not significantly influence the aeroelastic results.

Table 3 presents results from a linear calculation for flutter frequency and speed for the present wing model. As above, the results from the present analysis are obtained with all nonlinear effects suppressed. These are compared against the results obtained using theory of Ref. 12, which uses a Rayleigh-Ritz structural analysis with uncoupled beam mode shapes and Theodorsen's 2-D thin-airfoil theory for unsteady aerodynamics. The results are practically identical, indicating that eight finite elements is sufficient for the purposes of aeroelastic flutter calculations where high-frequency effects are not important.

Nonlinear flutter results

What is meant by "nonlinear flutter" needs to be clarified. The complete nonlinear model is used to obtain the equilibrium configuration. Then, a flutter analysis is done for equations that are linearized about the equilibrium configuration. Fig. 1 presents the nonlinear flutter results for the wing model including deformation due to gravity and aerodynamic forces. There are rapid changes in the flutter speed at low values of α_0, the root angle of attack. The nonlinear flutter speed and frequency are much lower than those estimated by the linear model. At around 0.61° there is a jump in the flutter speed and frequency. After the jump there is a smooth decrease in flutter speed and frequency. At around 4.5° the flutter speed again jumps, this time off the scale of the plot. Fig. 2 shows the tip displacement at the flutter speed. There is a discontinuity in the tip displacement which coincides with that in Fig. 1. A small but finite tip displacement is favorable for flutter for this configuration.

Flutter speed and tip displacement

It turns out that there is a strong relationship between the wing-tip displacement and the flutter speed. In the example considered above, the drastic change in aeroelastic characteristics is due to changes in the structural characteristics of the wing due to bending (tip displacement). Unfortunately, this effect was somewhat confused due to additional velocity-tip displacement coupling introduced by α_0. Apart from flutter speed being a function of tip displacement, the tip displacement itself was a function of the speed of the aircraft.

In the case study presented in this section, the tip displacement is obtained by applying a tip load. The results for the structural frequencies versus wing-tip displacement are shown in Fig. 3. One observes a large decrease in the modal frequency for a coupled torsion/edgewise bending mode as tip displacement is increased. The flatwise bending modes are unaffected. Fig. 4 shows the corresponding drop in both flutter speed and flutter frequency with increase in tip displacement. To understand the results presented in the previous section one needs now to do cross-matching.

Fig. 5 demonstrates how closely the wing tip displacement correlates with the flutter speed for various values of α_0 (Fig. 1). The thick line plots the flutter speed with tip displacement (same as Fig. 4). The other curves plot the tip displacement due α_0 at various speeds. For example, the solid line for $\alpha_0 = 0^\circ$ is just a straight line because the tip displacement is only due to gravity. For very small α_0, the flutter and tip displacement curves intersect at very small speeds and one gets very low flutter speeds. For slightly higher α_0 around 0.5° the flutter and tip displacement curves intersect three times. Thus, one observes that the wing flutters in a range of speeds, after which it is again stable for a range of speeds, after which it flutters again. The first range of flutter speeds however decreases with increasing α_0. At around $\alpha_0 = 0.75^\circ$, the first two intersection points collapse, the slopes of these curves are the same for a given value of α_0, and the flutter speed jumps to the next flutter range. For a tip displacement of around -1.5 m, one sees a jump in the flutter speed from approximately 22 m/s up to about 28 m/s, and a corresponding jump in frequency and tip displacement.

So, the nonlinear effects related to flutter might boil down to the fact that the natural frequencies shift around due to the changing equilibrium configuration about which the equations are linearized to obtain the nonlinear flutter solution. This corresponds to the decrease in the flutter speed shown in Fig. 1. The results in this section qualitatively explain the aeroelastic behavior shown in Fig. 1. To get better quantitative results one would need to have the exact displacement shape matching.

The jump in flutter speed at $\alpha_0 = 4.5^\circ$ in Fig. 1 can also be explained by similar matching. Fig. 6 shows the frequency and damping plots for larger angles of attack. Again, flutter occurs in a small range above the flutter critical speed. Though the flutter speed is decreasing with α_0, the strength and range of flutter is also decreasing. At around 4.5° the damping does not reach zero before reversing its direction and increasing.

Trim results

Fig. 7 shows the trim angle of attack, $\overline{\alpha}_0$ at various flight speeds. Contrary to expectations based only on linear static aeroelasticity, the value of $\overline{\alpha}_0$ required from a flexible wing is more than that from a rigid one. This is due to large flatwise bending which causes the lift, which is perpendicular to the flow and the wing reference line, to not act in the vertical direction. The displacement along the wing is certainly outside the region of applicability of linear theory, as indicated in Fig. 8 which shows the displacement shape of the wing at 25 m/s forward speed trim condition. This high deformation and associated loss of aerodynamic force in the vertical direction leads to the requirement of a higher value of $\overline{\alpha}_0$.

Fig. 9 plots the ratio of total lift (force in vertical direction perpendicular to the flight velocity and span) to rigid lift. The drastic loss of effective vertical lift is clearly observed as compared to linear results. The main significance of this result lies in the fact that, if stall angle is around 12°, then the rigid-wing analysis gives the stall speed to be 20 m/s, whereas the actual flexible aircraft would stall even at much higher flight speed of around 25 m/s. This would mean reduction in the actual flight envelope.

Rigid aircraft flight dynamics

Table 4 shows the the phugoid- and short-period-modal frequencies and dampings obtained by the present analysis, assuming a rigid wing. These results are compared against the frequencies obtained by the simple rigid aircraft analysis given in Roskam.[13] One sees that results from the present analysis are essentially identical to published results.

	Present Analysis	Analysis of Ref. 13	% Diff.
Phug. Freq. ω_{n_P}	0.320	0.319	+0.3
Phug. Damp. ζ_P	0.0702	0.0709	-1.0
S.P. Freq. $\omega_{n_{SP}}$	5.47	5.67	-3.5
S.P. Damp. ζ_{SP}	0.910	0.905	+0.6

Table 4: Comparison of rigid aircraft flight dynamics

Stability of complete aircraft

When flexibility effects are taken into account in the flight dynamic analysis, the behavior is distinctly different from that of a rigid aircraft. Fig. 10, compares the flight dynamics frequencies obtained with and without wing flexibility. The phugoid as well as the short period mode are affected by wing flexibility.

On the other hand, flight dynamic roots affect the aeroelastic behavior of the wing. Fig. 11 compares the root locus plot for the complete aircraft with those obtained by using linear wing aeroelastic analysis and nonlinear wing aeroelastic analysis. The nonlinear wing aeroelastic analysis uses the known flight trim angle of attack. A magnified plot is inserted which shows in these qualitative differences in more detail. It is clear that the low-frequency modes which involve flexibility are completely coupled to the flight dynamic modes changing the behavior completely. On the other hand, the high-frequency modes, one of which linear analysis predicts to be unstable at 34.21 m/s, are only affected by the nonlinearity. Thus if the trim solution is properly taken into account then the nonlinear wing analysis gives a good estimate of the actual wing plus aircraft combination modes.

Concluding Remarks

A nonlinear aeroelastic analysis has been conducted on a complete aircraft model representative of the current High-Altitude Long-Endurance (HALE) aircraft. Due to the large aspect ratio of the wing, the corresponding large deflections under aerodynamic loads, and the changes in the aerodynamic loads due to the large deflections, there can be significant changes in the aeroelastic behavior of the wing. In particular, significant changes can occur in the natural frequencies of the wing as a function of its tip displacement which very closely track the changes in the flutter speed. This behavior can be accounted for only by using a rigorous nonlinear aeroelastic analysis.

The overall flight dynamic characteristics of the aircraft also change due to wing flexibility. In particular, the trim solution, as well as the short-period and phugoid modes, are affected by wing flexibility. Neglecting the nonlinear trim solution and the flight dynamic frequencies, one may find the predicted aeroelastic behavior of the complete aircraft very different from the actual one.

Acknowledgments

This work was supported by the U.S. Air Force Office of Scientific Research (Grant number F49620-98-1-0032), the technical monitor of which is Maj. Brian P. Sanders, Ph.D. The Daedalus model data provided by Prof. Mark Drela (MIT) is gratefully acknowledged.

References

[1] Patil, M. J., Hodges, D. H., and Cesnik, C. E. S., "Nonlinear Aeroelastic Analysis of Aircraft with High-Aspect-Ratio Wings," In *Proceedings of the 39th Structures, Structural Dynamics, and Materials Conference*, Long Beach, California, April 20 – 23, 1998, pp. 2056 – 2068.

[2] Dunn, P. and Dugundji, J., "Nonlinear Stall Flutter and Divergence Analysis of Cantilevered Graphite/Epoxy Wings," *AIAA Journal*, Vol. 30, No. 1, Jan. 1992, pp. 153 – 162.

[3] Tang, D. M. and Dowell, E. H., "Experimental and Theoretical Study for Nonlinear Aeroelastic Behavior of a Flexible Rotor Blade," *AIAA Journal*, Vol. 31, No. 6, June 1993, pp. 1133 – 1142.

[4] Virgin, L. N. and Dowell, E. H., "Nonlinear Aeroelasticity and Chaos," In Atluri, S. N., editor, *Computational Nonlinear Mechanics in Aerospace Engineering*, chapter 15. AIAA, Washington, DC, 1992.

[5] Gilliatt, H. C., Strganac, T. W., and Kurdila, A. J., "Nonlinear Aeroelastic Response of an Airfoil," In *Proceedings of the 35th Aerospace Sciences Meeting and Exhibit*, Reno, Nevada, Jan. 1997.

[6] van Schoor, M. C. and von Flotow, A. H., "Aeroelastic Characteristics of a Highly Flexible Aircraft," *Journal of Aircraft*, Vol. 27, No. 10, Oct. 1990, pp. 901 – 908.

[7] Waszak, M. R. and Schmidt, D. K., "Flight Dynamics of Aeroelastic Vehicles," *Journal of Aircraft*, Vol. 25, No. 6, June 1988, pp. 563 – 571.

[8] Pendaries, C., "From the HALE Gnopter to the Ornithopter - or how to take Advantage of Aircraft Flexibility," In *Proceedings of the 21st Congress of the International Council of the Aeronautical Sciences*, Melbourne, Australia, Sept. 13 – 18, 1998, A98 - 31715.

[9] Hodges, D. H., "A Mixed Variational Formulation Based on Exact Intrinsic Equations for Dynamics of Moving Beams," *International Journal of Solids and Structures*, Vol. 26, No. 11, 1990, pp. 1253 – 1273.

[10] Peters, D. A. and Johnson, M. J., "Finite-State Airloads for Deformable Airfoils on Fixed and Rotating Wings," In *Symposium on Aeroelasticity and Fluid/Structure Interaction, Proceedings of the Winter Annual Meeting*. ASME, November 6 – 11, 1994.

[11] Peters, D. A., Barwey, D., and Johnson, M. J., "Finite-State Airloads Modeling with Compressibility and Unsteady Free-Stream," In *Proceedings of the Sixth International Workshop on Dynamics and Aeroelastic Stability Modeling of Rotorcraft Systems*, November 8 – 10, 1995.

[12] Patil, M. J., "Aeroelastic Tailoring of Composite Box Beams," In *Proceedings of the 35th Aerospace Sciences Meeting and Exhibit*, Reno, Nevada, Jan. 1997.

[13] Roskam, J., *Airplane Flight Dynamics and Automatic Flight Controls*, Roskam Aviation and Engineering Corporation, Ottawa, Kansas, 1979.

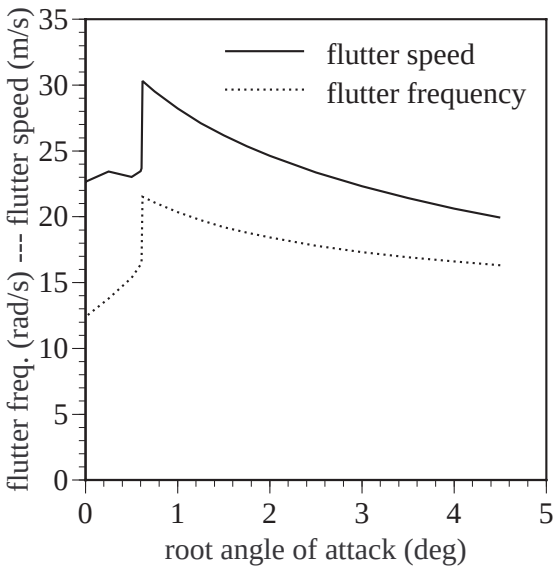

Figure 1: Variation of flutter speed with angle of attack

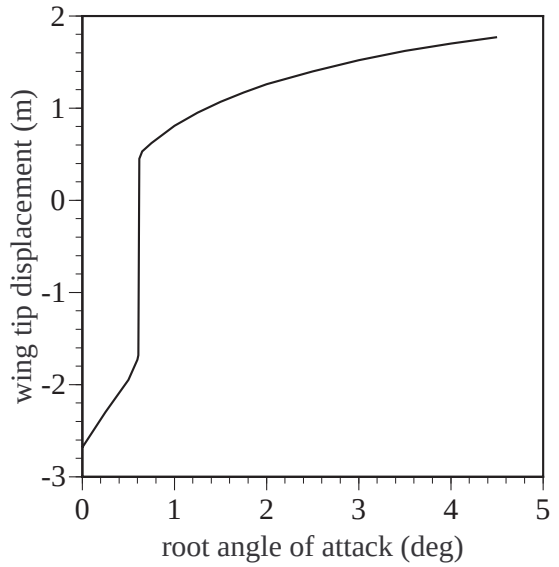

Figure 2: Flutter tip displacement at various root angles of attack

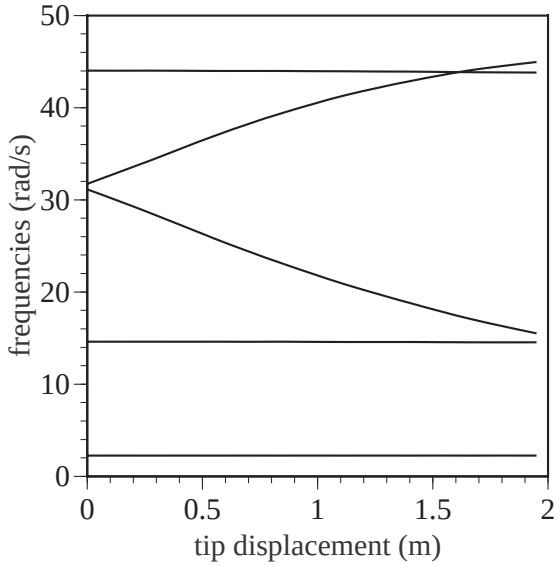

Figure 3: Variation of structural frequencies with tip displacement

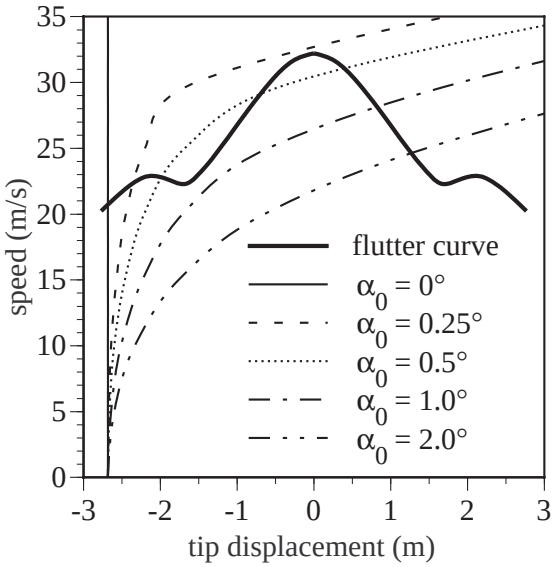

Figure 5: Correlation of flutter speed and wing tip displacement

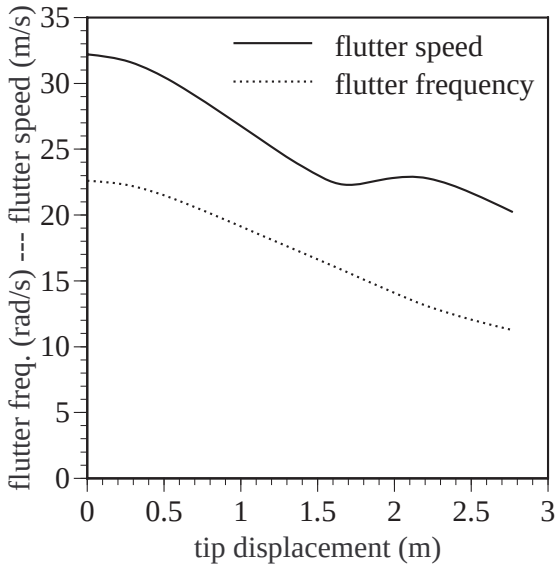

Figure 4: Variation of flutter speed and frequency with tip displacement

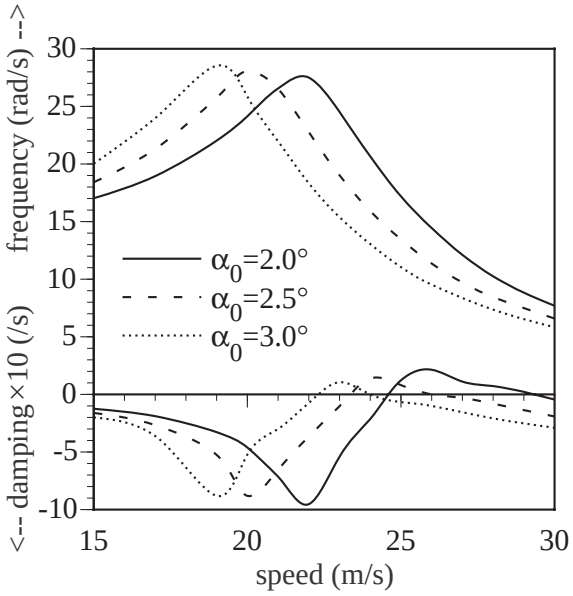

Figure 6: Flutter frequency and damping plots for various root angles of attack

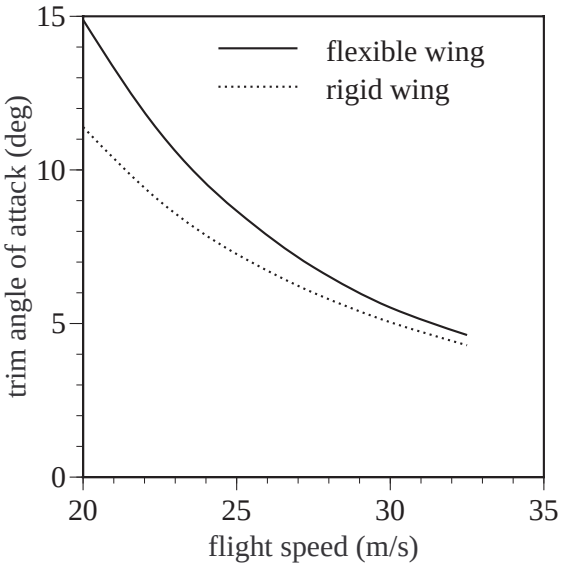

Figure 7: Variation of $\overline{\alpha}_0$ with flight speed

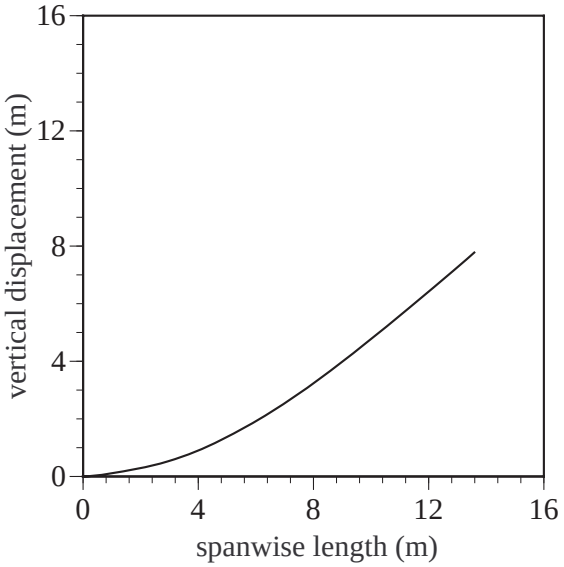

Figure 8: Wing displacement at 25 m/s

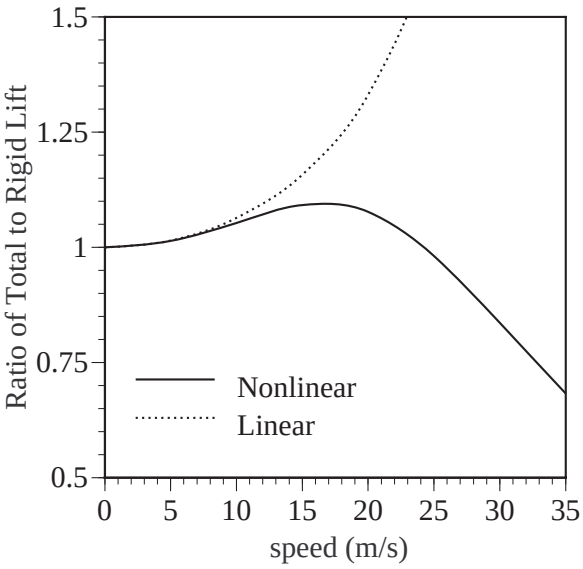

Figure 9: Total lift to rigid lift ratio at $\alpha_0 = 5°$

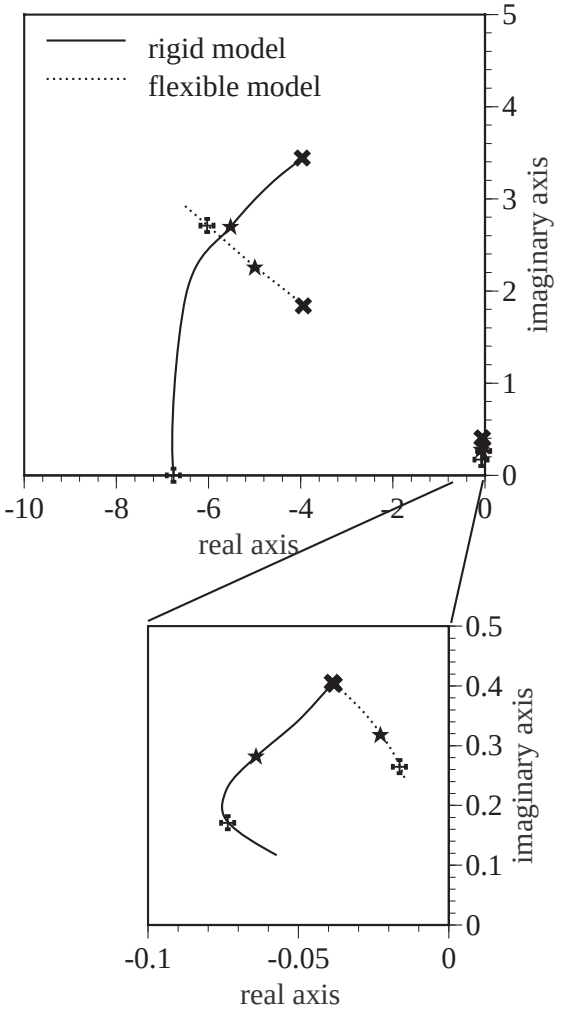

Figure 10: Root locus plot showing the flight dynamics roots, with a magnified section showing the roots nearest the origin

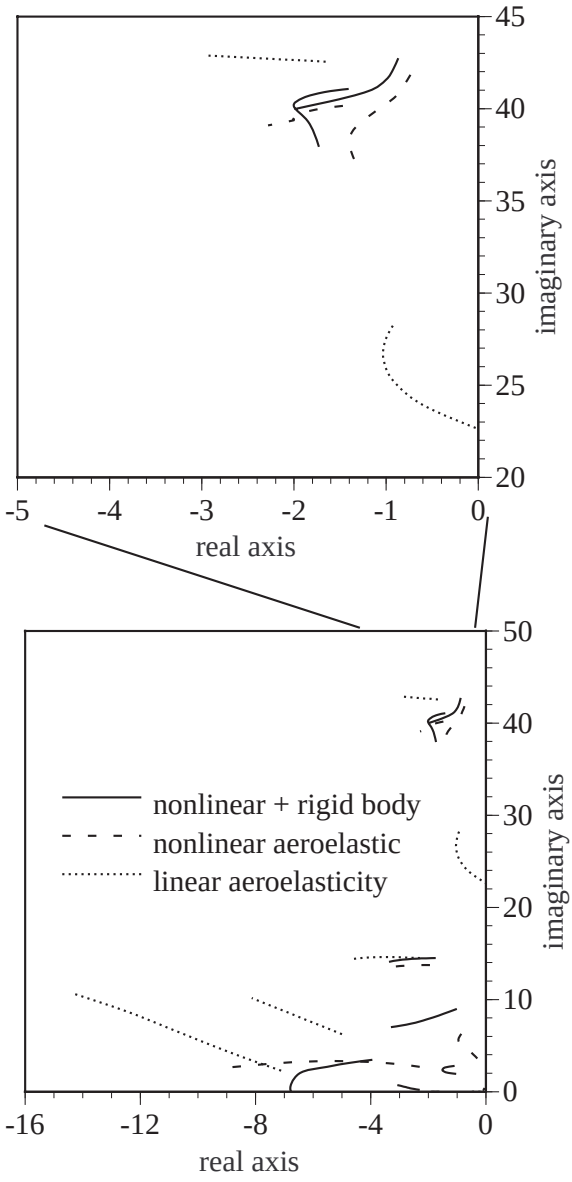

Figure 11: Expanded root locus plot with magnified section inserted which depicts roots in vicinity of the unstable root